

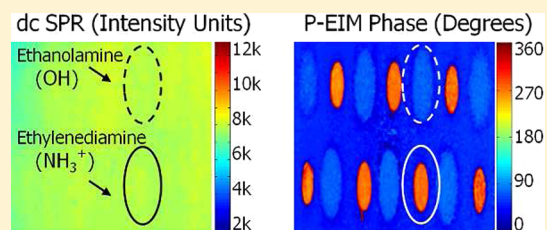
Charge-Based Detection of Small Molecules by Plasmonic-Based Electrochemical Impedance Microscopy

Christopher MacGriff,^{†,§} Shaopeng Wang,^{*,§} Peter Wiktor,[§] Wei Wang,[§] Xiaonan Shan,^{†,§} and Nongjian Tao^{†,§}

[†]School of Electrical, Computer, and Energy Engineering, Arizona State University, Tempe, Arizona 85287, United States

[§]Center for Bioelectronics and Biosensors, Biodesign Institute, Arizona State University, Tempe, Arizona 85287, United States

ABSTRACT: Charge-based detection of small molecules is demonstrated by plasmonic-based electrochemical impedance microscopy (P-EIM). The dependence of surface plasmon resonance (SPR) on surface charge density is used to detect small molecules (60–120 Da) printed on a dextran-modified sensor surface. Local variations in charge density on an electrode surface are manifest in an optical SPR signal. The SPR response to an applied ac potential measures the sensor surface impedance which is a function of the surface charge density. This optical signal is comprised of a dc and an ac component, and is measured with high spatial resolution. The dc element of the SPR signal represents conventional SPR imaging information. The amplitude and phase of local surface impedance is provided by the ac component. The phase signal of the small molecules is a function of their charge status, which is manipulated by the pH of a solution. Small molecules with positive, neutral, and negative charge are detected by P-EIM. This technique is used to detect and distinguish small molecules based on their charge status, thereby circumventing the mass limitation (~ 100 Da) of conventional SPR measurement.



The interactions between small molecules and biological macromolecules constitute a crucial component of biological networks and are the subject of extensive investigation in both academic and commercial laboratories. Important biological processes such as communication between cells, expression of genes, and immune response are dependent on massively parallel networks of the transient interactions of proteins and small molecules. Drug discovery and biomarker validation for clinical diagnosis rely on rigorous, quantitative measurements of binding events between small molecules and their biological receptors;¹ small molecules (generally <1000 Da) currently represent over 90% of FDA approved drugs.² The development of detection techniques for elucidating these types of binding reactions is paramount for the advancement of pharmacology and health therapeutics.

Current techniques to measure small molecule binding kinetics employ labels to detect the small molecule or its bound target, or alternatively, measure an intrinsic characteristic of the binding event or its constituent molecules in a “label-free” detection platform.^{3–6} The decision to use a particular measurement technique is informed by its inherent strengths and weaknesses, and the specific requirements for the intended measurement (e.g., sensitivity, selectivity, throughput, etc.). For example, the use of labels to enhance measurement sensitivity must be weighed against the potential consequence of adversely affecting the system being measured.^{7,8} By definition, label-free methods eschew this risk but may suffer from other limitations such as weak signals and nonspecific binding.⁹

We have previously developed label-free detection methods using plasmonic-based impedance imaging and spectroscopy,

and demonstrated their potential for studying the binding of macromolecules including antigen/antibody binding events.^{10–14} In our most recent demonstration the real-time electrical impedance signal followed the kinetics of the protein association and dissociation process and was less prone to the various sources of noise in conventional SPR measurements (i.e., bulk refractive index changes, nonspecific adsorption).¹⁵

Here we present a novel label-free technique for detecting and imaging small molecules using plasmonic-based electrochemical impedance microscopy (P-EIM). The molecules’ charge is expressed in the phase component of the electrochemical impedance, and therefore small molecules with charge different than the substrate can be detected with distinct phase signals. In addition, charge status of small molecules and/or the substrate can be manipulated by changing solution pH, and therefore in principle, any small molecules can be detected regardless the charge status and mass of molecules.

We believe P-EIM is immediately useful for a variety of applications. It could be used to directly measure small molecule binding events that have traditionally generated too small a signal for high throughput label-free assays (e.g., drug discovery). The study of post-translational modification (PTM) is another potential application of P-EIM: for example, monitoring the change in charge status due to the addition of charged phosphate groups during a phosphorylation event.¹⁶

Received: February 12, 2013

Accepted: July 1, 2013

Published: July 1, 2013



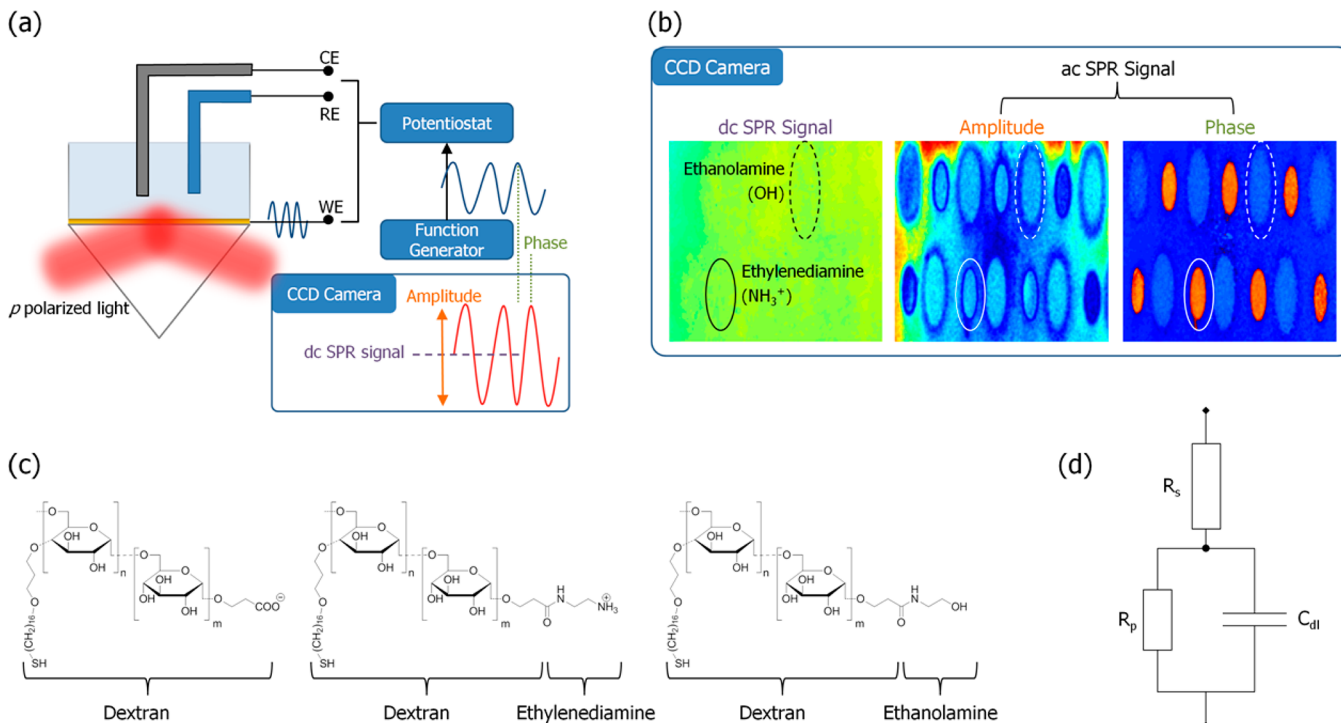


Figure 1. (a) Schematic illustration of the P-EIM setup. An ac potential modulation from a function generator is applied to the Au sensor chip (WE) via a potentiostat. (b) The P-EIM signals of printed small molecules spots (ethylenediamine and ethanolamine conjugated to dextran surface via EDC/NHS coupling chemistry, indicated by solid and dash circles, respectively) are imaged by a CCD camera, and vary with the applied voltage. The dc component of the response is the average intensity, and the ac component is comprised of a phase (relative to the applied potential) and amplitude (peak-to-peak amplitude). (c) Molecular structures of the charged dextran/small molecule conjugates. (d) The Randles equivalent circuit is used to model the electrical response of the sensor chip. The solution has a resistive effect (R_s), and the double layer formed on the interface between the sensor surface and solution (where the small molecules bound to) has both resistive (R_p) and capacitive (C_{dl}) characteristics.

EXPERIMENTAL SECTION

Materials. 16-Mercaptohexadecan-1-ol, epichlorohydrin, diethylene glycol dimethyl ether (diglyme), dextran, bromoacetic acid, *N*-(3-dimethylaminopropyl)-*N'*-ethylcarbodiimide hydrochloride (EDC), ethanol, ethanolamine, ethylenediamine dihydrochloride (ethylenediamine), NaOH, H₂SO₄, and Na₂CO₃ were purchased from Sigma (St. Louis, MO).

Chip Preparation. The Au sensor chips were rinsed with water and ethanol then annealed with hydrogen flame. The chips were treated with a 5×10^{-3} M solution of 16-mercaptopentadecan-1-ol in a 4:1 ethanol to water solution overnight at 25 °C. The resulting hydrophilic surfaces were then reacted with a 0.6 M solution of epichlorohydrin in a 1:1 mixture of 0.4 M sodium hydroxide and diglyme for 4 h at 25 °C. After being thoroughly washed with water, ethanol, and water again, the chips were treated with a basic dextran solution (3 g of dextran in 10 mL of 0.1 M sodium hydroxide) for 20 h at 25 °C. Further functionalization of the carboxymethyl-modified matrix was done by reaction with bromoacetic acid (1 M solution in 2 M sodium hydroxide) for 20 h at 25 °C. The dextran-modified sensor chips were rinsed with water, dried with nitrogen gas, and stored at 4 °C under nitrogen gas.

Small Molecule Printing. Stock solutions (1 M) of water mixed with ethylenediamine and ethanolamine, respectively, were prepared preceding the print. Both of these small molecules have at least one amine group, which is used for their immobilization to the dextran surface via EDC coupling. A sample of 20 μL of each solution was mixed with 20 μL of 0.8 M EDC in water immediately prior to printing. The solutions were deposited at discrete spots on the dextran-modified gold

surfaces. A noncontact piezoelectric inkjet printer (Engineering Arts LLC) was used to deposit a uniform pattern of spots with 500-μm spacing. A short, 22.5 kHz, burst of 5 drops deposited ~0.5 nL of solution at each spot. Precise dew-point control was used during printing to mitigate evaporation of the spots. Relative humidity (65%) and temperature (24 °C) were precisely regulated inside the printing chamber. The gold surfaces were chilled to 21 °C, which is a few degrees above the dew-point temperature (17 °C), to prevent condensation. After printing, the gold surfaces were maintained with dew-point control for 50 min and then stored under argon gas at 4 °C. Two batches of two chips were prepared to mitigate any variability transmitted from unknown nuisance factors of the printing process.

The printed spots on the sensor surface represent areas of high small molecule concentration (Figure 5). The P-EIM signals from these regions of interest (ROIs) are determined by the intrinsic properties of the small molecules (i.e., charge status) and environmental factors such as their distributions of mass from the printing process. Additionally, as the small molecules are immobilized in a three-dimensional hydrogel, the underlying dextran infrastructure also influences their P-EIM responses. These spots are prudently referred to as ROIs to reflect the ambiguity of their local print density and distribution.

Plamonic-Based Impedance Measurements. A custom SPR measurement system based on the Kretschmann configuration was used for the following experiments. A temperature-controlled (TCLDM9, ThorLabs) LED (wavelength 670 nm, Hamamatsu) was used as a light source.

Reflected light from a BK7 triangular prism was collected by a CCD camera (Pike, Allied Vision Technologies) with a 2.5–10 \times variable magnification lens (Edmund Optics). The SPR sensor chips (44 nm gold on a 1.5 nm chromium layer) were fabricated by thermal evaporation at high vacuum (3×10^{-6} Torr) on BK7 glass cover slides. Four Au chips were prepared in two batches to block any unknown effects of chip fabrication. The Au sensor chip served as a working electrode (WE) while silver and platinum wires were used as reference (RE) and counter electrodes (CE), respectively (Figure 1a). A potentiostat (EG&G model 283 potentiostat/galvanostat, Princeton Applied Research) controlled the potential of the WE with respect to the CE. A 10 s ac potential modulation of 500 mV (dc offset of 100 mV) at a frequency of 10 Hz was applied to the sensor chip for each solution pH, and was controlled by an external function generator (model 33521A, Agilent). A PDMS gasket placed on top of the sensor surface formed an open well to house the solution and electrodes.

The pH of the solution was used to control the charge status of the printed small molecules and dextran surface. Three solutions were prepared at 0.5 mM: H₂SO₄ (pH 1), NaOH (pH 5), and Na₂CO₃ (pH 9). A low ionic strength is used to reduce the charge-screening effect of an electric double layer.¹⁷ The solution was removed via pipet prior to the addition of a subsequent solution. All three buffers were used for each of the four chips tested, and the run order of the buffer pH was randomized. The selection of the applied voltage amplitude, frequency, and offset potential were controlled via a homemade Matlab software. The camera output and potential modulation signals were captured by a data acquisition board (NI USB-6251, National Instruments) using the same Matlab program. A fast Fourier transform algorithm was applied to the SPR image data captured by the CCD camera to generate phase and amplitude information for the imaged sensor surface.

RESULTS AND DISCUSSION

Basic Principle and Setup. Conventional electrical impedance spectroscopy measures the electrical current response (ΔI) of an electrode surface to an applied ac potential modulation (amplitude ΔV applied at frequency ω) to determine surface impedance ($Z(\omega) = \Delta V/\Delta I$). In contrast, P-EIM does not require electrical current measurement; the principle of P-EIM is based on the dependence of the SPR signal ($\Delta\theta$) on the surface charge density ($\Delta\sigma$) of the sensor. We have previously shown that $\Delta\theta$ is proportional to $\Delta\sigma$, given by $\Delta\sigma = \alpha\Delta\theta$, where α is a coefficient that can be calibrated experimentally or calculated theoretically.⁸ The current density (ΔJ) on the sensor surface is related to charge density by $\Delta J = j\omega\Delta\sigma$ (where $j = -1^{1/2}$). Therefore, the local surface impedance density can be determined by the ac component of the SPR signal ($\Delta\theta$) as given by $Z(\omega) = j\omega\alpha\Delta\theta/\Delta V$.

The measured response of the P-EIM technique is simply an optical signal of light intensity, varying sinusoidally with time due to the modulation of applied electrical potential. The dc component is the average intensity of this signal and represents conventional SPR measurement; it is a function of the local refractive index on, and immediately above, the sensor surface. The ac signal has an amplitude and phase (or equivalently, real and imaginary parts) which represent the electrochemical impedance density on the sensor surface. The dc and ac SPR signals are simultaneously measured to provide high-resolution SPR imaging and electrochemical impedance imaging capabilities in the same setup.

Effect of Solution pH. The charge status of a small molecule ROI is determined by the protonation status of the immobilized molecules' terminal functional groups, which is a function of the pH of the solution (Table 1). The respective

Table 1. Charge Status of Small Molecule Terminal Groups as a Function of Solution pH

molecule	solution pH		
	1	5	9
ethanolamine	OH	OH	OH
dextran	COOH	COO ⁻	COO ⁻
ethylenediamine	NH ₃ ⁺	NH ₃ ⁺	NH ₂

pK_A values of ethylenediamine and ethanolamine were determined from the Curtipot program.¹⁸ The unbound end of the printed ethanolamine regions are terminated with OH functional groups and remain neutral in the pH range of the tested solutions. At a pH below 3.5, the dextran surface does not carry a charge; the COOH terminal groups remain neutral.¹¹ The unbound end of the immobilized ethylenediamine is terminated with one amine group, which carries a positive charge (NH₃⁺) at the low solution pH. As the pH of the solution increases, the terminal groups on the dextran surface become negatively charged (COO⁻). The positively charged amine groups are neutral (NH₂) at pH 9 and the ethylenediamine ROIs lose their positive charge.

Impedance Models. The impedance response of the sensor can be described by an electrical model by using a Randles equivalent circuit and a mechanical model of the three-dimensional dextran hydrogel response (Figures 1d, 2, and 3).

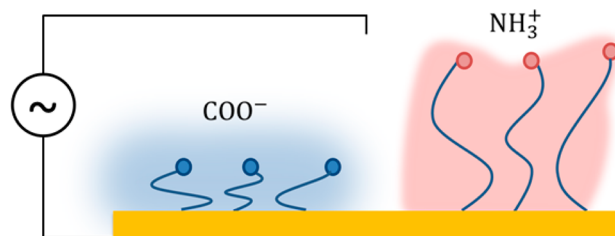


Figure 2. Illustration of the mechanical response of the dextran surface (blue lines). The solution pH determines the charge status of the terminal groups (dots). In general, the presence of charge increases the force from the applied potential on the dextran surface, resulting in greater amplitudes of fluctuation. Regions with positive charge respond 180° out of phase relative to negatively charged ROIs.

The solution is understood to have a resistive effect (R_s), and the double layer formed on the interface between the sensor surface and solution has both resistive (R_p) and capacitive (C_{dl}) characteristics. We have previously derived the relationships of these three electrical components and only list their final form here.⁹ According to the model, the current amplitude and phase on the sensor surface is given by:

$$I_{amp} = \left| \frac{\Delta V}{R_s + (R_p^{-1} + j\omega C_{dl})^{-1}} \right|$$

$$I_{phase} = \text{Arg} \left(\frac{\Delta V}{R_s + (R_p^{-1} + j\omega C_{dl})^{-1}} \right)$$

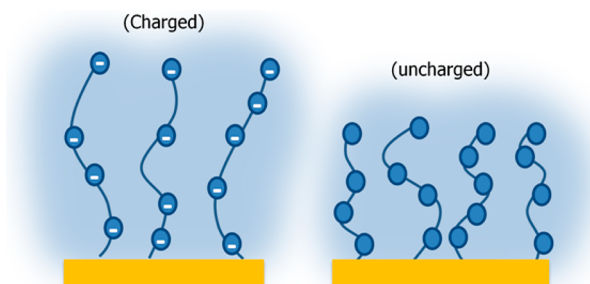


Figure 3. The repulsive electrical force between the charged terminal groups causes the dextran to expand (left). Dextran is more rigid in this state, decreasing the amplitude of SPR fluctuation. However, the presence of charge allows the hydrogel to respond to the driving ac potential, possibly increasing its amplitude of SPR fluctuation.

The modification of the sensor surface with a flexible dextran hydrogel adds an additional layer of complexity to the impedance model, as the hydrogel responds mechanically to the driving force of the ac potential. This response to the applied potential can be modeled as a driven harmonic oscillator with a spring constant that changes as a function of charge density.

The mechanical response of the dextran hydrogel on the sensor surface can be modeled as a viscoelastic medium driven by the force from the applied potential ($F \rightarrow = \pm qE \rightarrow$; the charged functional groups of the hydrogel and small molecule ROIs are displaced ($x = x_0 e^{-j\omega t}$) by the electric field according to the polarity of their charge (Figure 2). The mechanical response of the flexible hydrogel layer to the electrostatic driving force is described by k , the elastic restoring force constant, and γ , the internal damping of the polymer matrix. The corresponding equation takes the form of:

$$j\omega x_0 e^{-j\omega t} + kx_0 e^{-j\omega t} = \pm q\vec{E}$$

The displacement of a local region on the surface is described by:

$$x = \frac{\pm q\vec{E}}{\gamma j\omega + k}$$

Regions with a high density of charge experience an additional repulsive force between similarly charged functional groups, causing the hydrogel to become more rigid (Figure 3). This rigidity is the equivalent of a change in k .

The parameters in the Randles model are related to the viscoelastic model, but an explicit expression requires further information and assumptions. For example, the small molecules are not immobilized with a 100% printing efficiency; not every dextran terminal group in a small molecule ROI is used to bind the small molecule. The impedance response of the small molecule ROIs is influenced by these uncoupled carboxyl groups. Quantitative analysis of the absolute impedance signal is thus difficult but fortunately unnecessary for the purposes of small molecule detection. We consider the relative differences in impedance response between the different small molecule ROIs and dextran background. Due to the convolution of effects outlined above, we choose to focus on the phase component of the impedance signal, which follows the simple model of charge-based response.

Amplitude Component. At pH > 3.5, the terminal groups of the dextran hydrogel have a net negative charge. These

localized charges repel each other and cause the dextran to expand above the sensor surface. The reorganization of mass away from the sensor surface is confirmed by the decreased dc SPR signal at high pH (Figure 5). In this charged state the dextran surface is rigid and resists modulation by the applied potential. As explained above, the presence of charge has the additional effect of increasing the mechanical dextran response to the applied potential, which theoretically increases the amplitude of its fluctuation. As the number of negatively charged terminal groups increases, the hydrogel experiences a larger force from the applied potential and the dextran impedance decreases. At low pH the impedance-damping effect of rigidity is reduced but the uncharged dextran matrix experiences a smaller force from the applied voltage. The relationship between these two competing forces obfuscates the net impedance response of dextran and does not allow for an unambiguous interpretation of the amplitude component of the P-EIM signal.

Note that the presence of the small molecules (undetected by the conventional SPR signal) is easily confirmed by their amplitude signals (Figures 4 and 5). However, the phase responses of differently charged small molecules are much clearer, and allow for distinction based on charge status.

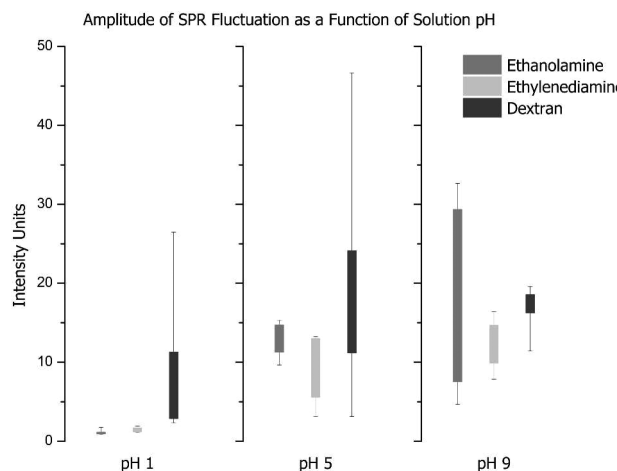


Figure 4. Box plots of pixel intensity of small molecule and dextran ROIs in the P-EIM amplitude images (filled boxes represent 25%–75% of mean values, minimum and maximum values marked by whiskers). The amplitude component of the P-EIM signal does not demonstrate any obvious patterns of SPR fluctuation for the small molecules or dextran ROIs.

Phase Component. A small molecule ROI's phase response is a function of its charge status and environmental effects such as the response of the underlying dextran matrix. The determination of the absolute phase signal is confounded by the multivariable response of the dextran hydrogel, and ultimately unnecessary. In the presence of an ac electric field, positively charged regions will respond up to 180° out of phase with negatively charged regions according to the oscillator model. The relative phase contrast of the differently charged regions is sufficient to detect and identify the small molecules.

At low pH, the positively charged ethylenediamine ROIs respond approximately 90° out of phase relative to the neutral ethanolamine and dextran regions. At pH 5, the positively charged ethylenediamine ROIs are 180° out of phase with the negatively charged dextran matrix. When the ethylenediamine

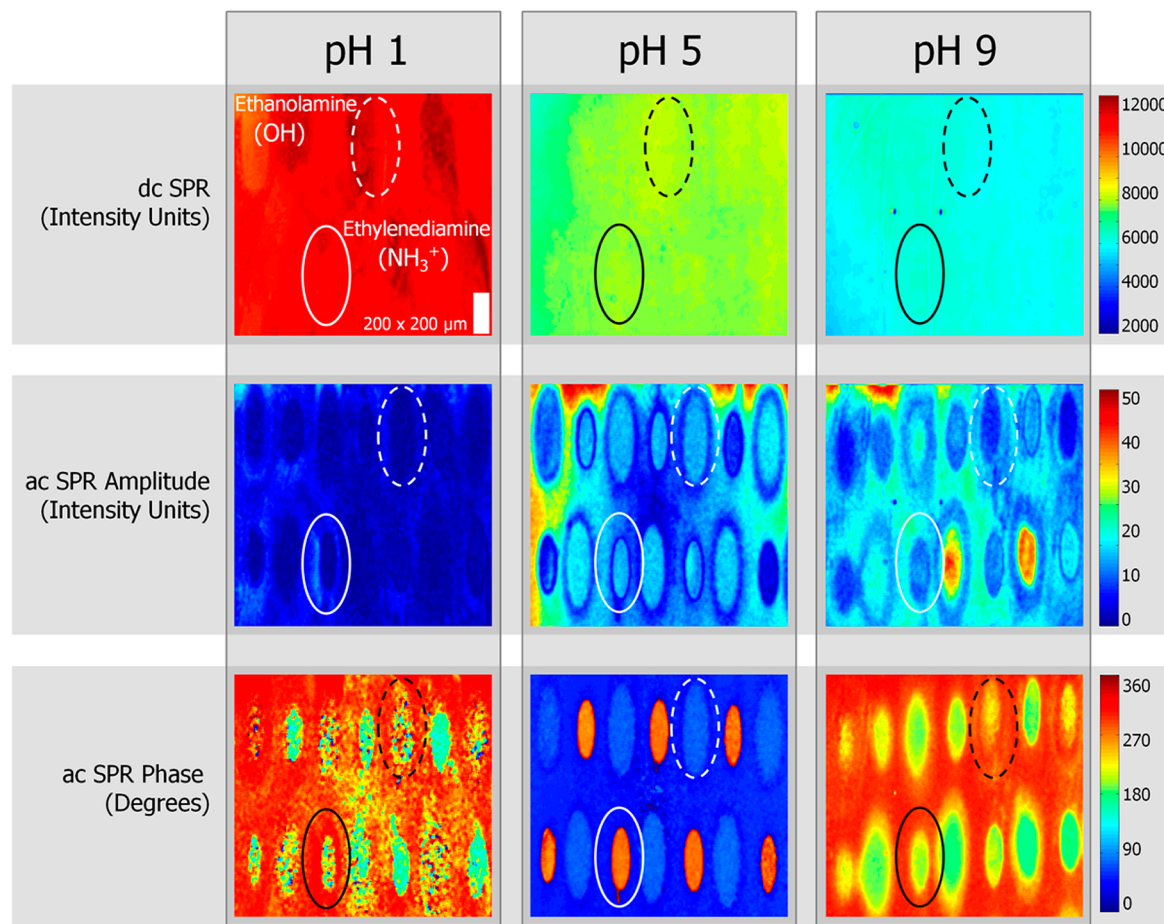


Figure 5. Dc and ac SPR signals as a function of solution pH. Ethanolamine and ethylenediamine are printed in an alternating pattern with 500 μm spacing on a dextran-functionalized Au microscope slide. (Top) The masses of the immobilized ethanolamine and ethylene small molecules are too small (60–120 Da) to be detected by conventional dc SPR. (Middle) The amplitude component of the ac SPR signal reveals the presence of the small molecules, but does not differentiate between them in an obvious manner. (Bottom) The phase component clearly distinguishes the small molecules based on their charge status. At pH 1 the neutrally charged COOH terminal groups of the dextran background are 90° out of phase from the positively charged NH₃⁺ terminal groups of the ethylenediamine regions of interest (ROIs). The neutrally charged ethanolamine ROIs (OH) are also resolved but have a larger distribution of phase response. At pH 5 the dextran is negatively charged (COO⁻) and is 180° out of phase with the positively charged ethylenediamine ROIs. At pH 9 the ethylenediamine ROIs become neutral and the phase contrast between the neutral and charged ROIs returns to 90°.

regions lose their positive charge at high pH, the phase contrast between the neutral and negatively charged regions decreases to 90°. These results are summarized in Figure 6.

Ideally, the neutral charge status of the ethanolamine ROIs would remain unchanged as a function of solution pH. However, this would require a 100% printing efficiency in which every terminal group of the dextran matrix binds to an ethanolamine small molecule during the printing process. It is reasonable to assume that not every dextran terminal group is consumed during the print in the ethanolamine ROIs and that the remaining unmodified COOH regions follow the general trend of the global dextran matrix. The histogram plots of the ethanolamine regions tend to follow the dextran response, but their phase response never exceeds that of the dextran. The influence of the unmodified dextran terminal groups is greater in the neutrally charged ethanolamine than the ethylenediamine ROIs (which have positively charged terminal groups to screen the surrounding negative charge and present a net positive charge).

CONCLUSION

We have demonstrated that charge-based detection of small molecules is possible using plasmonic-based electrochemical impedance microscopy (P-EIM). The P-EIM phase signal was found to be a function of localized surface charge; the phase contrast between differently charged printed small molecules and a dextran hydrogel sensor surface was used to detect and identify the small molecules, and was validated by the pH dependence of the various ROIs' charge statuses. The technique requires that a small molecule target be differently charged than the binding or background surface, which can be achieved by control of solution pH and/or selection of proper probing/referencing molecules. Therefore this technique is applicable to small molecules with any charge status. More importantly, this "proof-of-principle" P-EIM measurement provides a mass independent signal that could potentially be used to measure post-translational modifications or small molecule binding events in drug discovery or clinical diagnostics.

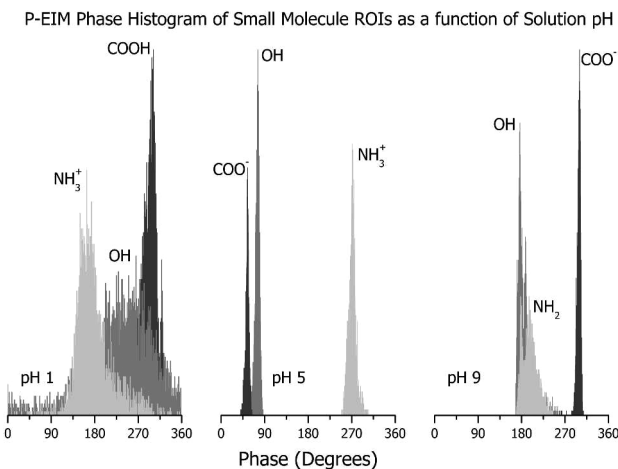


Figure 6. Pixel intensity histograms of small molecule and dextran ROIs in the P-EIM phase images. The P-EIM phase signal allows for the detection and identification of small molecules based on their charge status. At a solution of pH 1, regions with immobilized ethylenediamine (NH_3^+ functional groups) are approximately 90° out of phase with neutrally charged dextran (COOH) and ethanolamine (OH) ROIs. When the solution pH is increased above the pK_A of the dextran surface to pH 5, there is a 180° phase contrast between the positively charged functional groups of the ethylenediamine and the negatively charged carboxyl groups of dextran. At pH 9 the ethylenediamine functional groups lose their positive charge and are once again 90° out of phase with the negatively charged dextran ROIs.

AUTHOR INFORMATION

Corresponding Author

*E-mail: shaopeng.wang@asu.edu.

Notes

The authors declare no competing financial interests.

ACKNOWLEDGMENTS

Financial support from NSF grant 1151105, and Virginia Piper foundation is acknowledged.

REFERENCES

- (1) Krishnamoorthy, G.; Carlen, E. T.; van den Berg, A.; Schasfoort, R. B. M. *Sens. Actuators, B* **2010**, *148*, 511–521.
- (2) DrugBank 3.0: A comprehensive resource for ‘Omics’ research on drugs: Knox, C.; Law, V.; Jewison, T.; Liu, P.; Ly, S.; Frolkis, A.; Pon, A.; Banco, K.; Mak, C.; Neveu, V.; Djoumbou, Y.; Eisner, R.; Guo, A. C.; Wishart, D. S. *Nucleic Acids Res.* **2011**, *39*, D1035–41.
- (3) Haake, H. M.; Schutz, A.; Gauglitz, G. *Fresenius' J. Anal. Chem.* **2000**, *366*, 576–585.
- (4) Morgan, C. L.; Newman, D. J.; Price, C. P. *Clinical Chem.* **1996**, *42*, 193–209.
- (5) McNeil, C. J.; Athey, D.; Rennerberg, R. In *Frontiers in Biosensorics: Practical Applications*; Scheller, F. M., Schubert, F., Fedrowitz, J., Eds.; Birkhäuser: Basel, Switzerland, 1997; pp 17–25.
- (6) Skladal, P. *Electroanalysis* **1997**, *9*, 737–745.
- (7) Ray, S.; Mehta, G.; Srivastava, S. *Proteomics* **2010**, *10*, 731–748.
- (8) Espina, V.; Woodhouse, E. C.; Wulfkuhle, J.; Asmussen, H. D.; Petricoin, E. F., III; Loitza, L. A. *J. Immunol. Methods* **2004**, *290*, 121–133.
- (9) Wassaf, D.; Kuanga, G.; Kopacz, K.; Wu, Q.-L.; Nguyen, Q.; Toews, M.; Cosic, J.; Jacques, J.; Wiltshire, S.; Lambert, J.; Pazmany, C. C.; Hogan, S.; Ladner, R. C.; Nixon, A. E.; Sexton, D. J. *Anal. Biochem.* **2006**, *351*, 241–253.
- (10) Foley, K. J.; Shan, X.; Tao, N. *J. Anal. Chem.* **2008**, *80*, 5146–5151.
- (11) Shan, X. N.; Patel, U.; Wang, S. P.; Iglesias, R.; Tao, N. *J. Science* **2010**, *327*, 1363–1366.
- (12) Wang, S. P.; Huang, X. P.; Shan, X. N.; Foley, K. J.; Tao, N. *J. Anal. Chem.* **2010**, *82*, 935–941.
- (13) Wang, W.; Foley, K.; Shan, X.; Wang, S. P.; Eaton, S.; Nagaraj, V. J.; Wiktor, P.; Patel, U.; Tao, N. *J. Nat. Chem.* **2011**, *3*, 249–255.
- (14) Shan, X.; Wang, S.; Wang, W.; Tao, N. *J. Anal. Chem.* **2011**, *83*, 7394–7399.
- (15) Lu, J.; Wang, W.; Wang, S.; Shan, X.; Li, J.; Tao, N. *J. Anal. Chem.* **2012**, *84*, 327–333.
- (16) Cohen, P. *Nat. Cell Biol.* **2002**, *4*, E127–E130.
- (17) Shan, X.; Huang, X.; Foley, K. J.; Zhang, P.; Chen, K.; Wang, S.; Tao, N. *J. Anal. Chem.* **2010**, *82*, 234–240.
- (18) Gutz, I. G. R. (2012). *Curtipot program, Version 3.6.1, pH and Acid-Base titration curves: Analysis and Simulation* [Online].